Available online at www.sciencedirect.com
SCIENCE DIRECT®
International Journal of Heat and Mass Transfer 48 (2005) 4435–4445
International Journal of HEAT and MASS TRANSFER
www.elsevier.com/locate/ijhmt

The onset of thermal instability of a two-dimensional hydromagnetic stagnation point flow

Mustapha Amaouche [a], Faïçal Nait Bouda [a], Hamou Sadat [b,*]

[a] Laboratoire de physique théorique, Université de Béjaïa, Route de Targua Ouzemour Béjaïa, Algeria
[b] Laboratoire d'Etudes Thermiques, Université de Poitiers, 40 Avenue du Recteur Pineau, 86022 Poitiers, France

Received 15 November 2004; received in revised form 27 April 2005
Available online 12 July 2005

Abstract

The aim of the present paper is to examine the effects of a constant magnetic field on the thermal instability of a two-dimensional stagnation point flow. First, it is shown that a basic flow, described by an exact solution of the full Navier–Stokes equations exists under some conditions relating the orientation of the magnetic field in the plane of motion to the obliqueness of free stream. The stability of the basic flow is then investigated in the usual fashion by making use of the normal mode decomposition. The resulting eigenvalue problem is solved numerically by means of a pseudo spectral collocation method based upon Laguerre's functions. The use of this procedure is warranted by the exponential damping of disturbances far from the boundary layer and the appropriate distribution of the roots of Laguerre's polynomials to treat boundary layer problems. It is found through the calculation of neutral stability curves that magnetic field acts to increase the stability of the basic flow.

Keywords: Thermal instability; Hydromagnetic; Stagnation point; Laguerre's polynomials

1. Introduction

Magnetic fields are used in many practical situations that involve electrically conducting fluids in motion, like a liquid metal, electrolyte or plasma; they may substantially influence the fluid motion by interacting with the electric current induced in the fluid. Magnetic fields are employed, for example, to drive flows, induce stirring, levitation or to control heat transfer and turbulence. In the following, our concern is with the influence of a constant magnetic field on the convective flow near a two-dimensional stagnation point. We refer to this flow as the Hiemenz flow in hydromagnetics. Let us recall that boundary layer flow associated to a free stream impinging perpendicularly on a flat plate was first investigated by Hiemenz [1], who found an exact solution which is named after him. The mathematically attractive feature of the Hiemenz flow in hydromagnetics, unlike that in the classic Hiemenz flow, is that it represents, under some conditions, an exact solution of the incompressible continuity, energy and Navier–Stokes equations. Many aspects of the problem at hand have been discussed in the past [2–4], because of their occurrence in industrial applications such as nuclear engineering in connection with the cooling of reactors, heat exchangers design or cooling of electronic devices. As in many other configurations, magnetohydrodynamic

* Corresponding author. Tel.: +33 0549453543; fax: +33 0549453545.
E-mail address: hamou.sadat@univ-poitiers.fr (H. Sadat).

0017-9310/$ - see front matter
doi:10.1016/j.ijheatmasstransfer.2005.05.003

mechanisms affect not only the convective motion of the fluid, but also the stability of the flow. We are not aware of any work for this question in spite of its crucial importance.

In the absence of buoyancy and magnetic forces, it seems that this problem were first considered by Görtler [5] who derived the disturbance equations for the Hiemenz flow. These equations were studied by Hammerlin [6] who demonstrated that plane stagnation flow can sustain three-dimensional disturbances. The algebraic decay required at upstream infinity leads to solutions having a continuous spectrum of spanwise wavenumber. Hammerlin's result seems unsatisfactory because a unique eigenvalue would be expected. Kestin and Wood [7] conjectured that the inconclusive nature of Hammerlin's investigation is the result of the Hiemenz's idealization where the normal velocity component remains everywhere proportional to the normal coordinate. In the real case this velocity component starts out with that property but tends continuously to a constant value at upstream infinity. With this modification and by including certain small terms associated with the curvature of the wall, they predict the existence of a disturbance of unique wavelength corresponding to a regularly distributed system of counter rotating vortices. This result agrees well with their experimental observations and is fully consistent with the vortical structures exhibited in the flow visualization studies of Hodson and Nagib [8] and Sadeh and Brauer [9]. The problem was re-examined by Wilson and Gladwell [10], who argued that the remedy given by Kestin and Wood [7] is irrelevant and the correct solution may be derived from the disturbance equations proposed by Görther [5] together with a more stringent boundary condition at infinity. Wilson and Gladwell [10] proposed that the disturbance quantities must decay exponentially far upstream and they found then a discrete wave spectrum corresponding to stable solutions. Lyell and Huerre [11] developed linear and nonlinear analysis by using Galerkin expansion where the trial functions are the eigenfunctions of the potential stagnation point. They showed that the solution calculated by Wilson and Gladwell [10] constitutes the least damped mode of an infinite number of stable modes, and found that the linearly stable flow can be destabilized by disturbances of sufficiently high level. Nonlinear instability of Hiemenz flow was also found by Kerr and Odd [12] who, moreover, gave a new class of steady solutions to the Navier–Stokes equations, consisting in a periodic array of counter rotating vortices with the axes aligned with the streamwise direction. Nonlinearity is in fact one of the multiple mechanisms which may destabilize the stagnation point flow. For example, the introduction of unsteadiness into the mean flow is found by Thompson and Manly [13] to be a source of instability. The effect of blowing and the superposition of a sufficient crossflow in the free stream are also found by Hall et al. [14] to destabilize the stagnation point flow. When buoyancy alone is taken into account, computations of Chen et al. [15] have revealed that thermal excitation generates three-dimensional disturbances when the Rayleigh number exceeds some critical value. These authors found that the critical Rayleigh number and the critical wavenumber are relatively insensitive to the Prandtl number, when defined on the basis of the thermal boundary layer lengthscale. These findings remain qualitatively unchanged when obliqueness of the free stream [16] and the relative direction of buoyancy forces [17] are taken into account.

In the present contribution our main interest is with the interplay between magnetic and buoyancy forces. It will be shown that these mechanisms act to oppose each other; buoyancy is to destabilize the flow whereas magnetic effects are to increase its stability.

2. Analysis

2.1. Equations of fluid motion

We consider an electrically conducting fluid impinging obliquely on a hot flat plate, kept at a constant temperature T_w, and lying in the (x^*, z^*) plane which can be, without loss of generality, considered horizontal. The y^* axis is normal to the plate and pointing towards the flow. The latter is submitted to the action of an external uniform magnetic field **B**, arbitrarily oriented in the (x^*, y^*) plane as shown on Fig. 1. In addition to the usual MHD (magnetohydrodynamic) approximations, we will assume that the magnetic Reynolds number which is a measure of the ratio of magnetic convection to magnetic diffusion, is much less than unity. This indicates that the magnetic field is practically unmodified by the flow, whereas the former can control the latter very strongly on a laboratory scale. Further, we will assume that the induced electric field is negligible (see Appendix A). This corresponds to the case where no energy is added to (or extracted from) the fluid by electrical means. So, the electric term is not included in the relevant equations and only the applied magnetic field plays a role. Moreover, Joule heating and Hall effects are ignored. Hence, making use of the Boussinesq approximation, the equations of mass, momentum and energy conservation may be expressed, in terms of the temperature T and velocity **v**, as

$$\nabla \cdot \mathbf{v} = 0 \tag{1}$$

$$\mathbf{v_t} + (\mathbf{v} \cdot \nabla)\mathbf{v} + \frac{\nabla p}{\rho} = \nu \nabla^2 \mathbf{v} - \mathbf{g}\beta(T - T_\infty) + \frac{\sigma}{\rho}(\mathbf{v} \wedge \mathbf{B}) \wedge \mathbf{B} \tag{2}$$

$$T_t + (\mathbf{v} \cdot \nabla)T = \frac{\nu}{Pr}\nabla^2 T \tag{3}$$

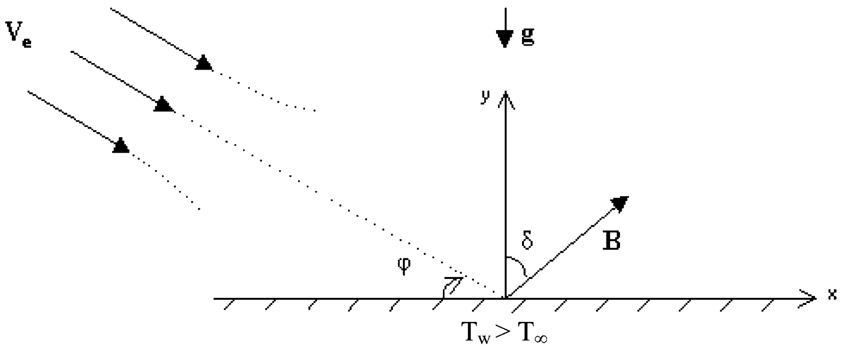

Fig. 1. Schematic representation of the problem.

to be solved with the boundary conditions

$$\mathbf{v}(x^*,0) = \mathbf{0}, \quad T(x^*,0) = T_w \tag{4}$$

$$\mathbf{v}(x^*,y^*) = \mathbf{v}_e(x^*,y^*), \quad T(x^*,y^*) = T_\infty \quad \text{as } y^* \to \infty \tag{5}$$

Here, p is the pressure, $\mathbf{g}$ is the gravity field, T_∞ is the ambient temperature, ρ, v, β, σ and Pr are the constant physical properties of the fluid, namely the mean density, kinematic viscosity, coefficient of thermal expansion, electrical conductivity and Prandtl number, respectively. Finally, $\mathbf{v}_e = (ax^* + by^*, -ay^*, 0)^t$ indicates the external velocity which can be interpreted as a combination of a linear shear flow, with constant shear stress b, parallel to the streamwise direction and a potential stagnation point flow characterized by the constant a.

2.2. The basic flow

In order to seek a basic, steady and two-dimensional solution, Eqs. (1) and (2) can be advantageously rewritten using stream function formalism. Taking the curl of Eq. (2) allows to eliminate the pressure and the following set of equations is then obtained.

$$\psi_y(\nabla^2\psi)_x - \psi_x(\nabla^2\psi)_y - \nabla^2(\nabla^2\psi) + Gr\theta_x + Ha^2(\sin^2\delta\psi_{xx} + \sin(2\delta)\psi_{xy} + \cos^2\delta\psi_{yy}) = 0 \tag{6}$$

$$\nabla^2\theta + Pr(\psi_x\theta_y - \psi_y\theta_x) = 0 \tag{7}$$

The boundary conditions take the form

$$\psi(x,0) = \psi_y(x,0) = \theta(x,0) - 1 = 0 \tag{8}$$

$$\theta(x,\infty) = 0, \psi(x,y) = xy\sin\gamma + \frac{1}{2}y^2\cos\gamma \quad \text{as } y \to \infty \tag{9}$$

The above equations are, for convenience, phrased in terms of dimensionless variables. Distances (along the plate and normal to it) and time are scaled using the factors $\ell = v^{1/2}(a^2+b^2)^{-1/4}$ and $(a^2+b^2)^{-1/2}$, respectively. The streamfunction ψ is referred to v and the scaled temperature is defined by $\theta = (T - T_\infty)/(T_w - T_\infty)$. The angle γ such that $\gamma = \arctan(a/b)$ gives the obliqueness of the external flow, which is related to the angle ϕ at which ψ vanishes as $y \to \infty$ by $\gamma = \arctan(\tan\varphi/2)$. The parameters in the problem are the Hartmann number $Ha^2 = \sigma|\mathbf{B}|^2\ell^2/\mu$ where μ is the magnetic permeability of the fluid and $Gr = |\mathbf{g}|\beta(T_w - T_\infty)\ell^3/v^2$. The present scaling, defined on the basis of the viscous scale length, is suitable for situations where the thermal boundary layer thickness is larger than the dynamic one. It is the case when the Prandtl number is small. The viscous scale remains appropriate as long as Pr is not too large (of order unity). However, since the instability is originated by buoyancy, a normalization based on the thermal boundary layer scale length ($\ell Pr^{-1/3}$) rather than the viscous scale length should be more suitable, especially for large Pr. The advantage of working with the dimensionless number Gr is that it may be interpreted as a Grashof number related to the scale length ℓ as well as a Rayleigh number based on the thermal scale $\ell Pr^{-1/3}$. For these reasons, it constitutes a relevant indication for the problem at hand, especially for small and large Prandtl numbers. The relevance of this parameter was demonstrated by the numerical calculations of Chen et al. [15], who found that the critical value of Gr for the onset of instability tends to a finite limit as $Pr \to \infty$. To find basic solution to Eqs. (6)–(9), we exploit the underlying linearity, with respect to the streamwise coordinate, of the external stream function. Thus, the following forms are introduced:

$$\left.\begin{aligned} \psi(x,y) &= xf(y) + g(y) \\ \theta(x,y) &= h(y) \end{aligned}\right\} \tag{10}$$

Once these expressions are reported in Eqs. (6)–(9), one is led, after some manipulation, to a set of ordinary differential equations governing the functions f, g and h.

$$f'''' + ff''' - (f' + Ha^2\cos^2\delta)f'' = 0 \tag{11}$$

$$g'''' + fg''' - Ha^2\cos^2\delta g'' - f''g' = Ha^2\sin(2\delta)f' \tag{12}$$

$$h'' + Prfh' = 0 \tag{13}$$

to be solved together with the boundary conditions

$$f(0) = g(0) = f'(0) = g'(0) = 0, \quad h(0) = 1 \tag{14}$$

$$f'(\infty) = \sin\gamma, \quad g''(\infty) = \cos\gamma, \quad h(\infty) = 0 \tag{15}$$

where the prime denotes differentiation with respect to y. Eq. (11) indicates that the parallel component of the magnetic field would have no effect on the Hiemenz's component of the flow. The so called tangential component of the flow would be driven not only by the obliqueness of the external flow but also by magnetic forces, provided that $\delta \neq 0 \bmod(\pi/2)$. Several situations may then arise depending on whether these two mechanisms act to either favor or oppose each other. The phenomenon is physically similar to that described in [17] by taking into account buoyancy forces induced by the inclination of the plate with respect to the horizontal. Eq. (11) may be integrated once, leading to

$$f''' + ff'' + (\sin^2\gamma - f'^2) + Ha^2\cos^2\delta(\sin\gamma - f') = 0 \tag{16}$$

The integration constant is determined by taking the limit $y \to \infty$ and using the prescribed boundary condition. Performing a change of variables $Y = y(\sin\gamma)^{1/2}$, $f(y) = (\sin\gamma)^{1/2}F(Y)$, Eq. (16) takes the form

$$\begin{aligned} &F''' + FF'' + 1 - F'^2 + \widetilde{Ha}^2(1 - F') = 0 \\ &F(0) = F'(0) = 0, \quad F'(\infty) = 1 \end{aligned} \tag{17}$$

where the incidence of the free stream is dropped, $\widetilde{Ha}^2 = Ha^2\cos^2\delta/\sin\gamma$ is a modified Hartmann number (it is assumed that $\sin\gamma \neq 0$). Now we let Y–C_0, C_0 being a real constant to be determined numerically by solving (17), be the asymptotic behavior of F for large Y. Then setting $g(y) = G(Y)/\sin\gamma$ and integrating once Eq. (12) yields

$$\begin{aligned} &G''' + FG'' - (F' + \widetilde{Ha}^2)G' = Ha^2\sin(2\delta)F + C_2 \\ &G(0) = G'(0) = 0, \quad G''(\infty) = \cos\gamma \end{aligned} \tag{18}$$

Performing the limit $Y \to \infty$, Eq. (18) takes the form

$$C_2 = (Y - C_0)\cos\gamma - \left(1 + \widetilde{Ha}^2\right)Y\cos\gamma - Ha^2(Y - C_0)\sin(2\delta)$$

The term in Y must be zero in order that C_2 be a constant; this gives

$$\cos\delta(2\sin\delta\sin\gamma + \cos\delta\cos\gamma) = 0 \tag{19}$$

This means that the assumed form of solution does really exist if and only if the foregoing geometrical conditions (19) holds. Under that condition, one obtains

$$C_2 = (Ha^2\sin(2\delta) - \cos\gamma)C_0$$

and hence, Eq. (18) becomes

$$G''' + FG'' - (F' + \widetilde{Ha}^2)G' = Ha^2\sin(2\delta)(F + C_0) - C_0\cos\gamma \tag{20}$$

The case $\cos\delta = 0$ naturally does not present any interest because magnetic effects would not affect the flow. Then the relation (19) becomes

$$\cot\gamma + 2\tan\delta = 0 \tag{21}$$

which means that, for a given incidence of the free stream, a basic flow exists in the form (10), provided that the orientation of the magnetic field is so that $\delta = -\arctan(1/2\cot\gamma) \bmod \pi$. We observe that (i) the parallel component of the flow and heat transfer are fully enslaved to its Hiemenz's component, (ii) the linearity of Eq. (20) allows to decompose the function G into two pieces, $G = Ha^2\sin(2\delta)G_1 + \cos\gamma G_2$, so that

$$\begin{aligned} &G_1''' + FG_1'' - (F' + \widetilde{Ha}^2)G_1' = F + C_0 \\ &G_1(0) = G_1'(0) = 0, \quad G_1''(\infty) = 0 \end{aligned} \tag{22}$$

$$\begin{aligned} &G_2''' + FG_2'' - (F' + \widetilde{Ha}^2)G_2' = -C_0 \\ &G_2(0) = G_2'(0) = 0, \quad G_2''(\infty) = 1 \end{aligned} \tag{23}$$

Hence taking (21) into account, the basic stream function writes

$$\psi(x, y) = x(\sin\gamma)^{1/2}F(Y) + \cot\gamma\left[G_2(Y) - \widetilde{Ha}^2G_1(Y)\right] \tag{24}$$

2.3. Formulation of the eigenvalue problem

The strong dependence of the basic state on x in the problem at hand does not permit introduction of eigenmodes in x, in general. However, the introduction of the element of infinite extent in the spanwise direction to model the problem permits considering the flow as homogeneous in this direction. Consequently, an eigenmode ansatz may be introduced in z. Given in addition that the temporal and spatial operators in Eqs. (1)–(5) are separable, disturbance quantities may be represented by

$$\hat{\mathbf{q}}(x, y, z, t) = \mathrm{Re}\left\{\hat{\mathbf{Q}}(x, y)\exp(\mathrm{i}kz + \omega t)\right\} \tag{25}$$

where $\hat{\mathbf{Q}} = (\tilde{u}, \hat{v}, \hat{w}, \hat{p}, \hat{\theta})^{\mathrm{t}}$ are complex amplitude functions of three-dimensional small disturbances that are periodic in z. A solution $\mathbf{q}(x, y, z, t)$ to Eqs. (1)–(5) is then decomposed, in the usual way, into

$$\mathbf{q}(x, y, z, t) = \mathbf{q_b}(x, y) + \hat{\mathbf{q}}(x, y, z, t) \tag{26}$$

where $\mathbf{q_b} = (u, v, 0, p, \theta)^{\mathrm{t}}$ indicating the basic flow. The linear stability analysis consists in determining the complex wave numbers and frequencies of the waves that the system supports. In most stability studies either a purely temporal or spatial instability approach is taken. In the spatial (temporal) analysis, the frequency (wavenumber) is real and the wavenumber (frequency) is allowed to be complex. The limitations of adopting a purely spatial or temporal instability analysis were made clear with the introduction of the concepts of absolute and convective instability. It seems [18] that the choice of a temporal or spatial analysis can only be fixed after the behavior of both the wave number and frequency have been studied in the complex plane and the convective or absolute character of the instability has been determined. In the problem at hand it is customary to focus attention on temporal instability and in general it is assumed that ω is real. This assumption was verified by previous numerical investigations by allowing ω to be complex. Therefore, the marginal stability corresponds to a transcritical bifurcation ($\omega = 0$) with exchange of stability between two fixed points. However, this is not a general result. Indeed, Hall et al. [14] obtained complex values for ω by adding a crossflow. Both stationary and traveling crossflow disturbances were observed in experiments by Poll [19] and found numerically by Malik et al. [20] in a swept Hiemenz flow. Another interesting feature of the stability problem is that if special class of self similar solution analogous to (10) is considered for the disturbance amplitudes, a one dimensional eigenvalue problem is obtained. This observation, introduced by Görtler [5] and Hammerlin [6] for reasons of mathematical evidence, was analyzed by Hall et al. [14] and by Brattkus and Davis [21], who concluded that these modes were less stable compared to other modes. This so called Görtler model was extended for three-dimensional stability analysis by Criminale et al. [22] and Theofilis et al. [23]. In the problem at hand, unfortunately, it is easy to show that three-dimensional disturbances which have the same underlying similarity as the basic flow are no longer suitable to the analysis, for arbitrary γ and δ, since the resulting perturbation equations do not admit this class of disturbances as eigensolutions. In order that this form of solution works yet, we must take $\sin\delta = 0$ which yields, in view of Eq. (21), $\cos\gamma = 0$. Therefore, in connection with this, we will restrict ourselves to the Hiemenz's flow. Furthermore, it has been demonstrated [16,17] that the stability problem for the orthogonal case is qualitatively identical to the stability problem for the oblique case. There is yet no reasons to believe that this will not also be true for the hydromagnetic case, although this still needs to be verified. Hence, substituting the decomposition (26) into the incompressible continuity, energy and momentum equations yields, after linearization around the base state $\mathbf{q_b}$

$$\tilde{u}_x + \hat{v}_y + \hat{w}_z = 0 \tag{27}$$

$$(L - \nabla^2 + u_x + Ha^2)\tilde{u} + u_y \cdot \hat{v} + \hat{p}_x = 0 \tag{28}$$

$$(L - \nabla^2 - u_x)\hat{v} + \hat{p}_y - Gr \cdot \hat{\theta} = 0 \tag{29}$$

$$(L - \nabla^2 + Ha^2)\hat{w} + \hat{p}_z = 0 \tag{30}$$

$$(L - \nabla^2/Pr)\hat{\theta} + \theta_y \hat{v} = 0 \tag{31}$$

Homogeneous boundary conditions are required on $y = 0$ and as $y \to \infty$, here L denotes the linear operator $\partial_t + u\partial_x + v\partial_y$. Then using (25) and retaining the property of self similarity for the perturbation amplitudes

$$\hat{\mathbf{Q}}(x,y) = \left[x\hat{u}(y), \hat{v}(y), \hat{w}(y), \hat{p}(y), \hat{\theta}(y)\right]^{t} \tag{32}$$

the above system yields, after the elimination of the pressure $\hat{p}$ and transverse component of the velocity from Eqs. (27) and (30), an eigenvalue system of the form

$$\begin{pmatrix} \hat{L} - 3F' & -F'' & 0 \\ \hat{L}D & \hat{L}(D^2 - k^2) - k^2Ha^2 & -k^2Gr \\ 0 & -Prh' & D^2 + PrFD - k^2 \end{pmatrix} \begin{pmatrix} \hat{u} \\ \hat{v} \\ \hat{\theta} \end{pmatrix} = \omega \begin{pmatrix} 1 & 0 & 0 \\ D & D^2 - k^2 & 0 \\ 0 & 0 & Pr \end{pmatrix} \begin{pmatrix} \hat{u} \\ \hat{v} \\ \hat{\theta} \end{pmatrix} \tag{33}$$

where $D = \mathrm{d}/\mathrm{d}y$ and $\hat{L} = D^2 + FD + (F' - k^2 - Ha^2)\mathrm{Id}$, with Id being the identity operator.

This system is to be solved numerically in order to determine the eigenvalue ω along with the corresponding eigenfunctions $\hat{u}, \hat{v}$ and $\hat{\theta}$ as functions of the spanwise wave number k for the three parameters characterizing the overall fluid system and the base state, Gr, Pr and Ha. At marginality, corresponding to $\omega = 0$, only for some characteristic values of Gr will the problem allow a non trivial solution for given k, Pr and Ha. Once the critical conditions have been determined and the eigensolutions, which are defined modulo a multiplicative constant, representing the relevant variables of the marginal secondary flow calculated, the enslaved variables can be deduced from Eqs. (27) and (30). One obtains:

$$\begin{aligned} \hat{w} &= -\Im\mathrm{m}(\hat{u} + \hat{v}')/k \\ \hat{p} &= \quad \Im\mathrm{m}(\hat{L} - F')\hat{w}/k \end{aligned} \tag{34}$$

2.4. Computational method

In order to approximate the solution of the differential eigenvalue system to be solved and incorporate its exponential damping at infinity, we shall use a pseudo spectral method based on expansion by Laguerre's functions, i.e., Laguerre's polynomials $L_n(y)$ multiplied by a decaying exponential. So, truncating the expansion after a finite number N of terms, an approximation f_N of a function f is thought in the form $\Phi_N(y)\exp(-y)$ with Φ_N being a polynomial of degree at most N and forced to fulfill the linear system at collocation nodes which are selected to be the zeroes of $L_N(y)$. Several methods are available for their computation. In the Appendix B, the y_k are shown to be the eigenvalues of a certain matrix deduced from the well known recurrence formula. In spite of a "bad" value of the Lebesgue constant associated to the set y_k having $y_0 = 0$ as point of accumulation, correct result may be obtained for the approximation of functions possessing a certain rate of decay at infinity. Details about theory and numerical experiments and suggestions concerning the improvement of practical performances can be found in Madey et al. [24]. Some indications for numerical evaluations of the polynomial Φ_N are given below. We first express Φ_N in terms of Lagrange polynomials $G_k(y)$ with respect to the nodes y_k

$$\Phi_N(y) = \sum_{k=1}^{N} G_k(y)\Phi_N(y_k) \tag{35}$$

where $\Phi_N(y_k)$, $k = 1,\ldots,N$ are unknown coefficients to be determined.

The incorporation of the homogenous boundary condition on Φ_N at y_0 yields:

$$G_k(y) = \frac{yL_N(y)}{y_k(y-y_k)\frac{\mathrm{d}L_N}{\mathrm{d}y}(y_k)} \tag{36}$$

The values of the first derivative of $\Phi_N(y)$ at y_k may be related to the set $\Phi_N(y_k)$ from the formula (35). Furthermore the basic tool for the computation is the differential operator D_N in the space of polynomials of degree N.

$$D_N\Phi_N(y_k) = \sum_{n=1}^{N} d_{kn}\Phi_N(y_n) \tag{37}$$

The entries d_{kn} are given in the Appendix C. Similarly to (37), we get for higher derivatives:

$$D_N^m\Phi_N(y_k) = \sum_{n=1}^{N} d_{kn}^m\Phi_N(y_n) \tag{38}$$

The entries d_{kn}^m of the matrix associated to the operator D_N^{m} of order m can be deduced directly by successive derivation of (35) or more conveniently by successive application of the operator D_N according to (37). The latter needs the introduction of the polynomial $G_0(y) = L_N(y)$. Taking into account the homogenous boundary condition on $D\hat{v}$ at $y_0 = 0$, we get the following expression:

$$\begin{aligned} d_{kn}^2 &= \begin{cases} \sum_{l=1}^{N} d_{kl}d_{\mathrm{ln}}, & \text{if } D_N^2 \text{ is applied to } \hat{v} \\ \sum_{l=0}^{N} d_{kl}d_{\mathrm{ln}}, & \text{otherwise} \end{cases} \\ d_{kn}^3 &= \sum_{l=1,m=0}^{N} d_{km}d_{ml}d_{\mathrm{ln}} \\ d_{kn}^4 &= \sum_{l=1,p=0,m=0}^{N} d_{km}d_{mp}d_{pl}d_{\mathrm{ln}} \end{aligned} \tag{39}$$

In other words, introducing the $N \times N$ square matrices D_0 and $\widetilde{D}$ by the entries $d_{k0}d_{0n}$ and d_{kn} ($n \neq 0$, $k \neq 0$), respectively, the relations (39) express that the matrix $\widetilde{D}$ is associated to D_N, $\widetilde{D}^2$ or $\widetilde{D}^2 + D_0$ is associated to D_N^2 whether it is applied to $\hat{v}$ or not, $(D_0 + \widetilde{D}^2)\widetilde{D}$ and $(d_{00}I + \widetilde{D})D_0\widetilde{D} + (D_0 + \widetilde{D}^2)\widetilde{D}^2$ are associated to D_N^3 and D_N^4 respectively. Making use of (39), the discretization procedure transforms the original differential eigenvalue problem into an algebraic eigenvalue problem expressed in terms of discretization matrices $\mathbf{A}_1$ and $\mathbf{A}_2$ such that

$$\mathbf{A}_1(k, Pr, Gr, Ha)\Phi_N = \omega\mathbf{A}_2(k, Pr)\Phi_N \tag{40}$$

The problem is posed as a linear generalized eigenvalue problem for ω. In order that a nontrivial solution exists, the matrix $\mathbf{A}_1 - \omega\mathbf{A}_2$ must be singular. This allows to compute the ω spectrum for any combination of parameters k, Gr, Pr and Ha. The basic flow is then temporally unstable or stable whether there exists at least one positive eigenvalue or not. Instability occurs only above some level of heating given by the lowest value of Gr, obtained by varying the wavenumber, which cancels $\det\mathbf{A}_1$ at marginality.

3. Results and discussion

The stability characteristics of the flow are calculated by inverting the generalized algebraic eigenvalue problem using a standard IMSL subroutine. The results to be reported in this section are obtained by varying Ha and Pr. In order to achieve a satisfactory convergence, checks on the influence of the truncation level N were performed in terms of its effects on the basic flow and on the location of the critical conditions for the onset of instability. This showed that the accuracy of the numerical scheme can be improved by increasing the number of collocation nodes. However, higher accuracy is achieved at the expense of a significant increase in computational time. At least two decimal-point accuracy has been required in all of the numerical experiments. This accuracy is achieved by successively increasing N; convergence is assumed to be reached when further increase in N yields no further improvement in accuracy. A typical convergence test is displayed in Fig. 2 where the absolute value of the error ΔGr_c in the critical Grashof number is plotted versus the number of polynomials for various Ha and Pr. One can see that (i) the number of required polynomials increases by increasing Pr and Ha. This is in accordance with the fact that an increase in Pr and Ha reduces the boundary layer thickness; therefore a greater number of terms is needed in order to avoid spurious nodes and preserve the prescribed accuracy. (ii) Moderate values of these parameters ($Pr = 0.7$ and $Ha^2 = 10$) required only up to 40 terms while greater values ($Pr = 7$ and $Ha^2 = 20$) required more than 60 terms. An overview of the stability properties of the basic flow can be seen from the sequence of neutral stability curves displayed in Fig. 3 for (a) a typical value of Ha and varying values of Pr, (b) a typical value of Pr and varying values of Ha. Overall, these curves clearly depict that the onset conditions of instability are significantly affected by magnetic forces.

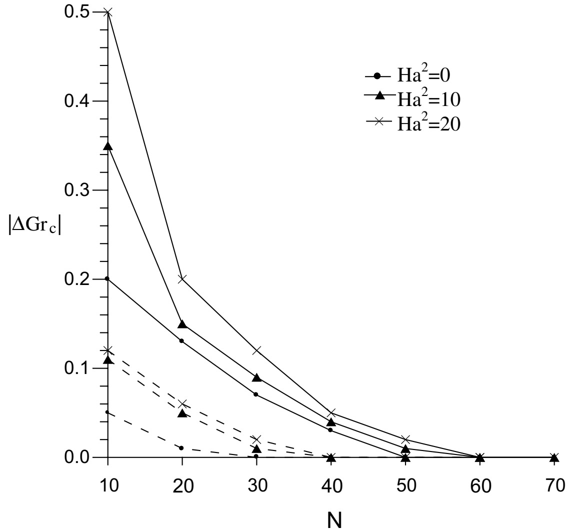

Fig. 2. Convergence test in terms of the absolute value of the error in the critical Grashof number versus the number of collocation nodes for: $Pr = 0.7$ (···) and $Pr = 7$(—) by varying *Ha*.

Specifically, the transition to secondary flow in the presence of magnetic forces occurs at a critical Grashof number that may be several times greater than the critical value for classical Hiemenz flow. For fixed value of *Pr*, results are qualitatively similar, indicating regular stabilization of the flow by magnetic forces and slight variations in the shape of the stability boundaries. For a given value of *Ha*, the instability region in the (k, Gr) plane is always and wholly contained in that corresponding to a smaller value of *Ha*. Fixing *Ha* and varying *Pr* globally produces an inverse effect; i.e., increasing *Pr* leads to the expansion of the instability region. As far as the onset of instability is concerned, a better global picture is provided by Fig. 4 showing (a) the critical Grashof number and (b) the wave number of the least stable mode, as functions of *Pr* and *Ha*. For a given *Ha*, one can observe from Fig. 4a that (i) Gr_c grows very rapidly as $Pr \to 0$, i.e., a little change in *Pr* greatly acts upon the instability threshold. (ii) The change in Gr_c becomes imperceptible to the change in *Pr* as $Pr \to \infty$. This observation is quite in accordance with the use of *Gr* as a relevant parameter for thermal instability, even in presence of magnetic forces. (iii) Gr_c reaches a minimum value (say $Gr_c = (Gr_c)_m$ for $Pr = Pr_m$) and varies slowly with *Pr* in an intermediate region, between a lower bound which is of unit order for all *Ha* and an upper one which depends on *Ha*. In that region, the effect of increasing *Pr* is destabilizing or stabilizing, depending on whether it is smaller or greater than the value Pr_m previously introduced. This threshold which marks the change in the qualitative influence of *Pr* is

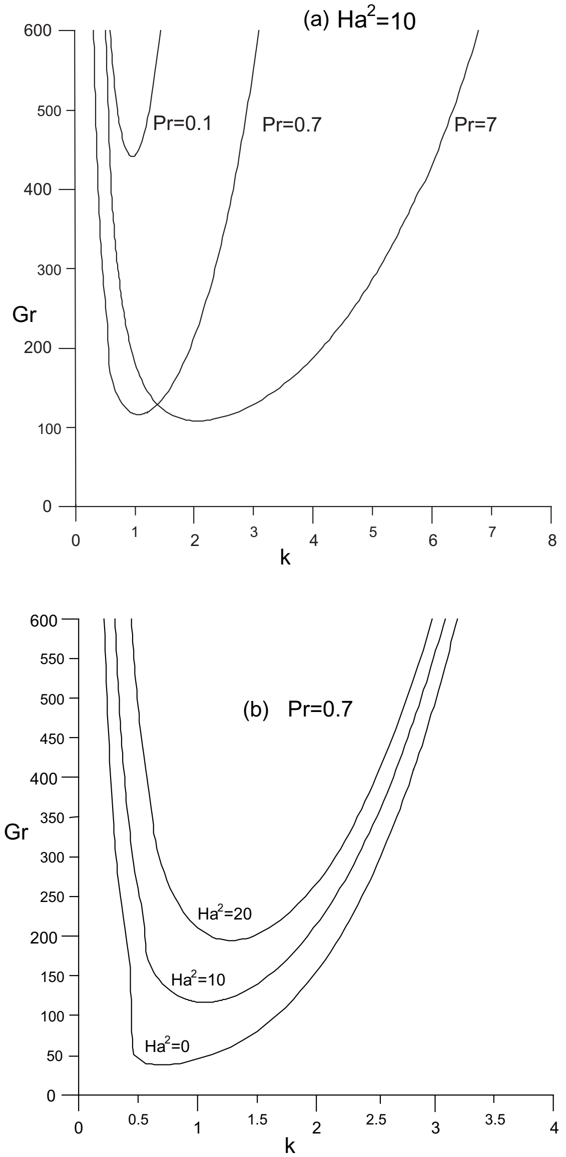

Fig. 3. Marginal stability diagram showing the wavenumber of the least stable mode versus the Grashof number for: (a) fixed values of *Ha* and varying *Pr*, (b) fixed *Pr* and varying *Ha*. The unstable region lies above the curve while the stable region lies below it.

close to unity for $Ha = 0$ and becomes larger with an increase in *Ha*. It can be expected that the physical meaning of the first two observations is related to the nature of the instability. For small values of *Pr*, thermal disturbances are prone to be dissipated as well as hydrodynamic disturbances. In other words, this means that buoyancy forces are sufficient to overcome inertia forces which make the system more stable. A greater amount of heating is therefore needed to destabilize the basic

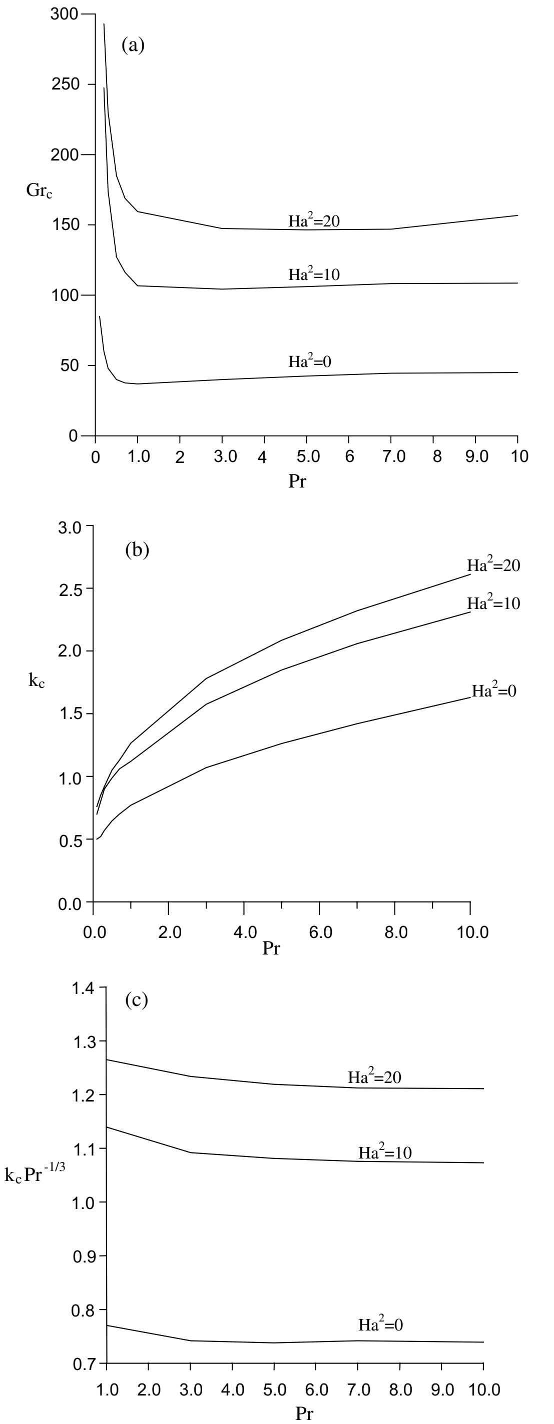

Fig. 4. Critical conditions for instability in terms of: (a) Grashof number (b) wavenumber referred to the viscous scale length (c) wavenumber referred to the thermal scale length, plotted versus *Pr* by varying *Ha*.

flow. On the other hand, as *Pr* increases the dissipation is reduced and the tendency to the destabilization is increased. The existence of the minimum value $(Gr_c)_m$ associated to Pr_m and therefore the non monotone decrease of Gr_c with *Pr* is apparently surprising. One expects that increasing *Pr* must produce a regular destabilization of the flow. A possible reason for this apparent anomaly is that the Grashof number does not quite constitute a relevant indication of thermal instability for intermediate value of *Pr*. A more suitable parameter must not only coincide with *Gr* for small and large values of *Pr*, but also would be such that its critical value decreases regularly by increasing *Pr*. This parameter would be a result of another scaling based on an intermediate scale length, between the viscous and thermal scales. Also, it can be seen from Fig. 4a that the effects of magnetic forces are to delay the onset of thermal instability. This is in conformity with the fact that magnetic and inertia forces act to favour each other and therefore *Pr* must be more important in order to increase thermal convection. Fig. 4b shows that both *Pr* and *Ha* act to increase the critical wavenumber. In fact the influence of sufficiently large values of *Pr* on k_c, may be simply expressed by introducing the thermal scale length. The variations of the corresponding critical wavenumber $k_c Pr^{-\frac{1}{3}}$ are reported in Fig. 4c. It is shown that the rescaled critical wavenumber does no longer depend on *Pr* for sufficiently large value of this parameter.

Results for the least stable and the most unstable branches are plotted in Fig. 5 which shows the temporal growth rate ω versus the wavenumber for $Pr = 0.7$ and two selected values of Ha^2 when (a) the thermal excitations are not yet sufficient to give rise to instability, i.e., $Gr < Gr_c$ and (b) the instability threshold is crossed, i.e., $Gr > Gr_c$. It is seen that an increase in Hartmann number leads to the attenuation of the most unstable and the least stable modes. This confirms that the effect of Hartmann number is to increase the stability of the flow. The stabilizing effect of magnetic field is obvious for values of k greater than approximately $k = 0.5$ and more effective just beyond $k = 0.5$; so it clearly plays a role in determining the k value where the growth rate peaks, selecting the wavelength of the most unstable mode.

Now, we calculate the steady secondary flow which arises from the transcritical bifurcation of the basic state at marginality in order to better understand the influence of Hartmann number on the onset of instability. Since, the equations and boundary conditions are homogeneous, the solution is determined apart from an arbitrary multiplicative factor that has to be made definite by imposing a normalization condition. We choose this to be $w(y_3) = 0.5$. The eigenfunctions of the critical mode, with and without magnetic field, are displayed in Fig. 6. We observe that the amplitudes of the velocity and temperature disturbances exhibit similar profiles in presence or not of magnetic field. This mean that, qualitatively, magnetic field does not significantly affect

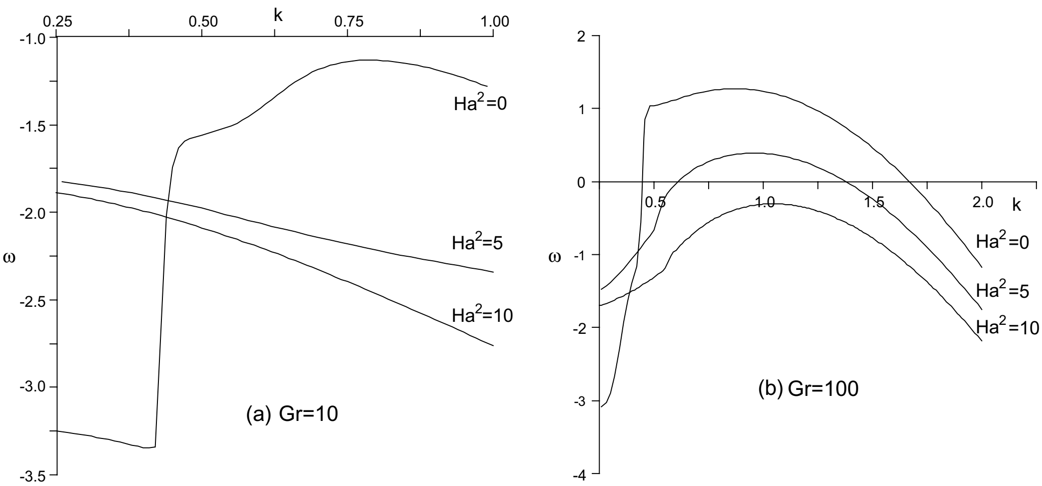

Fig. 5. Plot of the temporal growth rate versus the wavenumber for the least stable (or the most unstable) mode (a) before and (b) after the onset of instability; $Pr = 0.7$.

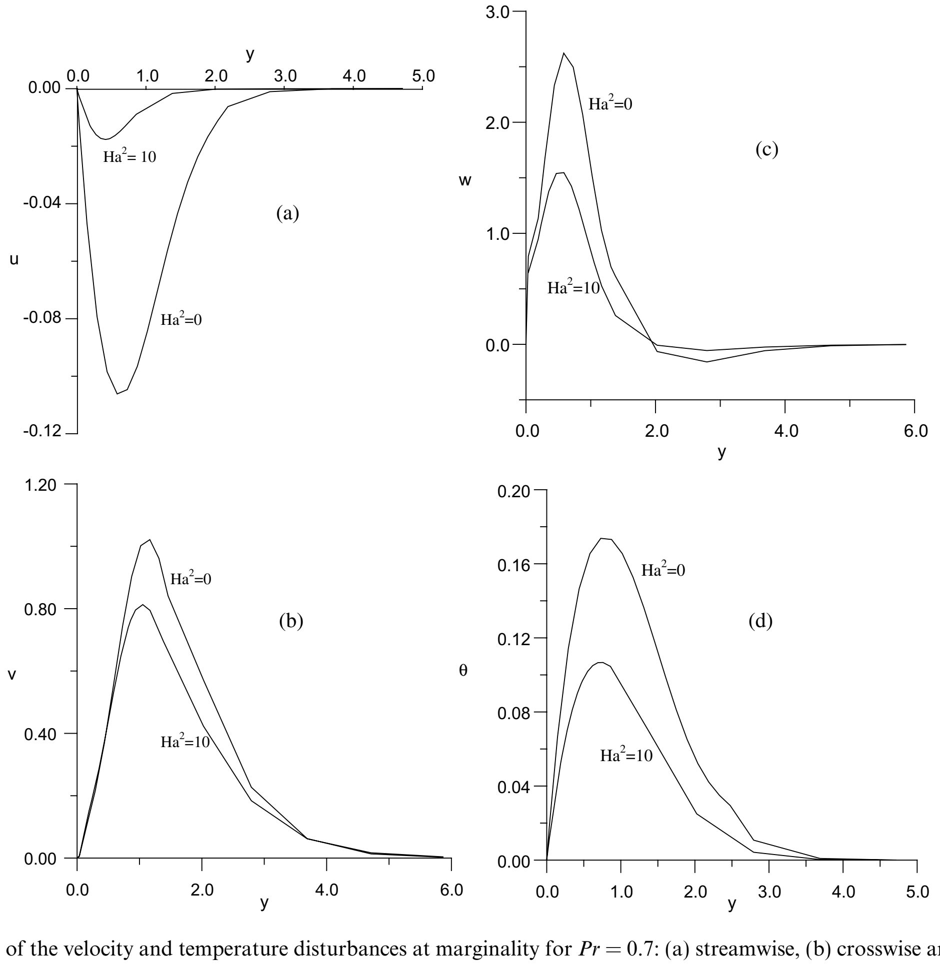

Fig. 6. Profiles of the velocity and temperature disturbances at marginality for $Pr = 0.7$: (a) streamwise, (b) crosswise and (c) spanwise velocity components, (d) temperature.

the secondary flow. In addition, theses profiles are relatively smooth which confirms that the number of collocations nodes used was sufficient. Most importantly, note that the effect of magnetic field is to reduce, as it can be expected, all of the eigenfunctions, and hence to oppose to the thermal instability.

4. Conclusion

The new insight into the study of two-dimensional hydromagnetic stagnation point flow gained by the results presented herein can be summarized as follows. First, it has been found that the direction of the applied magnetic field must be related to the obliqueness of the outer stream in order that an exact similarity solution exists for the basic flow. Regarding the stability problem, only that of the orthogonal flow can be described by the special class of self similar disturbances. In this case, increasing magnetic effects yields (i) the decrease of the temporal growth rate of the most unstable mode and of the least stable one, (ii) more important critical Grashof number for the onset of instability, (iii) the reduction of the region of instability in the (k, Gr) plane. This demonstrates the regularly stabilizing effects of magnetic forces.

Appendix A

The assumption of small magnetic Reynolds numbers allows us to neglect the induced magnetic field and yields $\mathbf{curl}\,\mathbf{E} = \mathbf{0}$. We have supposed as well that there is no excess charge density, which implies that the electric field is conservative ($\mathrm{div}\,\mathbf{E} = 0$). In addition to these two equations, the electric field must satisfy the following boundary conditions:

(i) $\mathbf{E} = \mathbf{0}$ along conducting boundaries provided that there is no prescribed polarization voltage (no electric potential jump between conducting boundaries).
(ii) along insulator boundaries, one has $J_n = 0$ (the index n indicates the normal component) which gives either $E_n = 0$ in the viscous fluid side owing to the adhesion condition or $E_n + (\mathbf{v_e} \wedge \mathbf{B})_n = 0$ when using the impermeability condition at the frontier of the inviscid fluid flow. In the latter case, observing that the velocity $\mathbf{v_e}$ is tangential to the boundary yields $E_n = 0$ when $\mathbf{B}$ is parallel to $\mathbf{v_e}$ or when the flow is two-dimensional, as it is the case in the problem at hand. In these conditions $\mathbf{E} = \mathbf{0}$ is the unique solution for the electrical equations.

Appendix B

The roots y_k of the Nth order Laguerre polynomial may be computed by solving the following eigenvalue problem.

$$\mathbf{M} \cdot \mathbf{L_k} = y_k \cdot \mathbf{L_k}$$

where

$$\mathbf{M} = \begin{bmatrix} 1 & -1 & & & & & & & \\ -1 & - & - & & & & & & \\ & - & - & - & & & 0 & & \\ & & - & - & - & & & & \\ & & & -n & 2n+1 & -(n+1) & & & \\ & & & & - & - & - & & \\ & & 0 & & & - & - & - & \\ & & & & & & - & - & 1-N \\ & & & & & & & 1-N & 2N-1 \end{bmatrix}$$

and

$$\mathbf{L_k} = \{L_0(y_k), \ldots, L_{N-1}(y_k)\}^{\mathrm{t}}$$

This is deduced from the well known recurrence formula

$$-nL_{n-1}(y) + (2n+1-y)L_n(y) - (n+1)L_{n+1}(y) = 0$$

by putting $y = y_k$, $n = 0, 1, \ldots, N-1$ and making use of $L_{-1}(y) = 0$ and $L_N(y_k) = 0$.

Appendix C

The derivation with respect to y of (36) gives:

$$\frac{\mathrm{d}G_n}{\mathrm{d}y}(y) = \begin{cases} \dfrac{\mathrm{d}L_N}{\mathrm{d}y}(y), \quad n = 0 \\ \dfrac{1}{(y-y_n)\frac{\mathrm{d}L_N}{\mathrm{d}y}(y_n)}\left(\dfrac{y}{y_n}\dfrac{\mathrm{d}L_N}{\mathrm{d}y}(y) - \dfrac{L_N(y)}{y-y_n}\right) \\ \quad n = 1, \ldots, N \end{cases}$$

By setting $y = y_k$, we get

$$d_{k0} = \begin{cases} -N, & k = 0 \\ -\dfrac{N}{y_k L_{N-1}(y_k)}, & k = 1, \ldots, N \end{cases}$$

$$d_{kn}(n = 1, \cdots, N) = \begin{cases} \dfrac{1}{Ny_n L_{N-1}(y_n)}, & k = 0 \\ \dfrac{1}{y_k - y}\dfrac{L_{N-1}(y_k)}{L_{N-1}(y_n)}, & k \neq 0, \ k \neq n \\ \dfrac{1+y_k}{2y_k}, & k = n \end{cases}$$

References

[1] K. Hiemenz, Die grenzschicht an einem in den gleichförmigen flüssigkeitsstrom eingetauchten geraden Kreiszylinder, Dingl. Polytech. J 326 (1911) 321–410.

[2] P.D. Ariel, Hiemenz flow in hydromagnetics, Acta Mech. 103 (1994) 31–43.

[3] M. Kuman, G. Nath, Flow and heat transfer in a stagnation point flow over a stretching sheet with magnetic field, Mech. Res. Commun. 26 (4) (1999) 469–478.

[4] T.C. Chiam, Heat transfer within variable conductivity in a stagnation point flow towards a stretching sheet, Int. Commun. Heat Mass Transfer 23 (1996) 239.

[5] H. Görtler, Dreidimensionale instabilität der abenen staupunktströmung gegenüber wirbelartigen strömungen, Füfzig jahre grenzschichtforschung Braunschweig, Vieweg und Sohn, 1955, pp. 304–314.

[6] G. Hammerlin, Zur Instabilitäts theorie der ebenen staupunktströmung, in: H. Görtler, W. Tollmein (Eds.), 50 jahre grenzschichtforschung, Vieweg und Sohn, 1955, pp. 315–327.

[7] J. Kestin, R.T. Wood, On the stability of two dimensional stagnation flow, J. Fluid Mech. 44 (1970) 461–479.

[8] P. Hodson, H. Nagib, Longitudinal vortices induced in a stagnation region by wakes-their incipient formation and effects on heat transfer from cylinders, IIT Fluids Heat Transfer Rep. R 75-2 (1975).

[9] W. Sadeh, H. Brauer, A visual investigation of turbulence in stagnation flow about a circular cylinder, J. Fluid Mech. 99 (1980) 53.

[10] S.D.R. Wilson, I. Gladwell, The stability of a two-dimensional stagnation flow to three dimensional disturbances, J. Fluid Mech. 84 (1978) 517–527.

[11] M.J. Lyell, P. Huerre, Linear and nonlinear stability of plane stagnation flow, J. Fluid Mech. 161 (1985) 295–312.

[12] O.S. Kerr, J.W. Dold, Periodic steady vortices in a stagnation point flow, J. Fluid Mech. 276 (1994) 307–325.

[13] C. Thompson, M.G. Manley, Linear stability of stagnation flow, Phys. Fluid A2 (1990) 1350–1363.

[14] P. Hall, M.R. Malik, D.I.A. Poll, On the stability of an infinite swept attachment line boundary layer, Proc. Roy. Soc. London Ser. A 395 (1984) 229–245.

[15] K. Chen, M.M. Chen, C.W. Sohn, Thermal instability of two dimensional stagnation point boundary layers, J. Fluid Mech. 132 (1983) 49–63.

[16] D.G. Lasseigne, T.L. Jackson, Stability of nonorthogonal stagnation flow to three dimensional disturbances, Theor. Comp. Fluid Dyn. 3 (1992) 207–218.

[17] M. Amaouche, D. Boukari, Influence of thermal convection on non-orthogonal stagnation point flow, Int. J. Therm. Sci. 42 (2003) 303–310.

[18] P. Moresco, J.J. Healey, Spatio temporal instability in mixed convection boundary layers, J. Fluid Mech. 402 (2000) 89–107.

[19] D.I.A. Poll, J. Fluid Mech. 150 (1985) 329.

[20] M.R. Malik, F. Li, C.L. Chang, Cross-flow disturbances in three dimensional boundary layers: nonlinear development, wave interaction and secondary instability, J. Fluid Mech. 268 (1994) 1–36.

[21] K. Brattkus, S.H. Davis, The linear stability of plane stagnation point flow against general disturbances, Q. J. Mech. Appl. Maths 44 (1991) 135–146.

[22] W.O. Criminale, T.L. Jackson, D.G. Lasseigne, Evolution of disturbances in stagnation point flow, J. Fluid Mech. 270 (1994) 331–347.

[23] V. Theofilis, A. Fedorov, D. Obrist, U.C. Dallmann, The extended Görtler–Hammerlin model for linear instability of three dimensional incompressible swept attachment line boundary layer flow, J. Fluid Mech. 487 (2003) 271–313.

[24] Y. Madey, B. Pernaud Thomas, H. Vandeven, Une réhabilitation des méthodes spectrales de type Laguerre, La recherche aérospatiale 6 (1985) 353–375.